

Article

# 3-[Bis(pyridin-2-ylmethyl)amino]-5-(4-carboxyphenyl)-BODIPY as Ratiometric Fluorescent Sensor for Cu<sup>2+</sup>

Akira Hafuka <sup>1,\*</sup>, Hisashi Satoh <sup>2</sup> , Koji Yamada <sup>3</sup>, Masahiro Takahashi <sup>2</sup> and Satoshi Okabe <sup>2</sup>

<sup>1</sup> Department of Integrated Science and Engineering for Sustainable Society, Faculty of Science and Engineering, Chuo University, 1-13-27 Kasuga, Bunkyo-ku, Tokyo 112-8551, Japan

<sup>2</sup> Division of Environmental Engineering, Faculty of Engineering, Hokkaido University, North-13, West-8, Sapporo 060-8628, Japan; qsatoh@eng.hokudai.ac.jp (H.S.); m-takaha@eng.hokudai.ac.jp (M.T.); sokabe@eng.hokudai.ac.jp (S.O.)

<sup>3</sup> Division of Environmental Materials Science, Graduate School of Environmental Science, Hokkaido University, North-10, West-5, Sapporo 060-0810, Japan; yamada@ees.hokudai.ac.jp

\* Correspondence: hafuka.14p@g.chuo-u.ac.jp; Tel.: +81-3-3817-7283

Received: 8 April 2018; Accepted: 14 May 2018; Published: 16 May 2018



**Abstract:** We developed an asymmetric fluorescent sensor **1** for Cu<sup>2+</sup>, based on 4,4-difluoro-4-bora-3a,4a-diaza-s-indacene (BODIPY), by introducing 4-carboxyphenyl and bis(pyridin-2-ylmethyl)amine groups at the 5- and 3-positions, respectively, of the BODIPY core. We then investigated the photophysical and cation-sensing properties of the sensor. BODIPY **1** showed large absorption and fluorescence spectral shifts on binding to Cu<sup>2+</sup>. The fluorescence peak at 580 nm red-shifted to 620 nm. The binding stoichiometry of BODIPY **1** and Cu<sup>2+</sup> was 1:3. The ratio of the fluorescence intensity at 620 nm to that at 580 nm ( $F_{620}/F_{580}$ ) increased with increasing concentration of Cu<sup>2+</sup> (3–10 equiv); this enabled ratiometric determination of Cu<sup>2+</sup>. Although BODIPY **1** showed good selectivity for Cu<sup>2+</sup>, there was an interfering effect of Fe<sup>3+</sup>. BODIPY **1** could be used for the naked-eye detection of Cu<sup>2+</sup> in a water-containing sample.

**Keywords:** boron-dipyrrromethene; di(2-picolyl)amine; cation; ion; copper; heavy metal; transition metal; dye; fluoroionophore; fluorescence

## 1. Introduction

The conservation of natural environments and their protection from hazardous contaminants are becoming considerably important. Heavy metals, in particular, have serious risks to the environment and to human health because of their toxicity. Copper (Cu) is one of the heavy metals, and excess uptake of Cu into the human body can lead to gastrointestinal disturbance, and liver or kidney damage [1]. The development of rapid and easy screening methods for heavy metals, including Cu, is therefore needed. Presently, the most general analytical methods for heavy-metal determination are inductively coupled plasma (ICP)-optical emission spectrometry, ICP-mass spectrometry, and atomic absorption spectrometry [2]. Although these analytical methods are precise and sensitive, they are costly, and always need complicated sample preparation. Furthermore, they are not used in on-site screening. The development of a cost-effective and easy method for determining concentrations of heavy metals is therefore necessary.

Fluorescence spectroscopy with fluorescent sensor molecules is an attractive method for quantifying heavy-metal cations, because of its high sensitivity, operational simplicity, and versatile instrumentation [3]. In addition, these sensor molecules can determine the free cation concentration of heavy metals, which is important in natural environments and many biological systems. The design and synthesis of new fluorescent sensor molecules are active areas of research, and different kinds

of fluorescent sensors for heavy-metal cations have been reported [4]. Among them, ratiometric fluorescent sensors that show fluorescence spectral shift caused by interaction with heavy-metal cations are more sensitive than those that show increase (“turn-on”) or decrease (“turn-off”) of fluorescence intensity [5]. Ratiometric fluorescent sensors enable reliable measurements of analyte concentrations, because the ratio of the intensities at two different fluorescence wavelengths is not affected by fluctuations in the source light intensity and concentration of the fluorescent sensor molecule.

Our strategy for the development of a ratiometric fluorescent sensor for heavy-metal cations is based on the synthesis of an asymmetric 4,4-difluoro-4-bora-3a,4a-diaza-*s*-indacene (BODIPY) fluorescent molecule with a cation receptor at the 3-position. BODIPY has many useful characteristics, such as narrow fluorescence and absorption spectrum, high fluorescence quantum yields, large molar absorption coefficients, and excellent photochemical stability [6]. In addition, BODIPY derivatives can be excited with visible light. The most distinctive characteristic of BODIPY derivatives is that their photophysical properties can be modified by appropriate substitution [7]. Among the eight positions on the BODIPY core, substitution at the 3- and/or 5-position(s) can cause significant shifts in the absorption and fluorescence spectra [7]. The introduction of a cation receptor at the 3- and/or 5- position(s) of BODIPY can therefore be used to create a ratiometric fluorescent sensor [8–13]. However, the development of a ratiometric fluorescent sensor for  $\text{Cu}^{2+}$  is difficult, because  $\text{Cu}^{2+}$  often shows fluorescence quenching with many fluorescent sensors, because of its paramagnetic nature [14–16]. In our previous study, we synthesized four types of 3-[bis(pyridin-2-ylmethyl)amino]-BODIPYs with bis(pyridin-2-ylmethyl)amine [di(2-picoly)amine] as the cation receptor at the 3-position of BODIPY [17]. We found that substitution with the electron-withdrawing sulfonylphenyl group at the 5-position gives the highest fluorescence quantum yield and largest absorption coefficient in the presence of  $\text{Cu}^{2+}$ . In this study, we introduced another type of electron-withdrawing group (i.e., a carboxyphenyl group) at the 5- position of 3-[bis(pyridin-2-ylmethyl)amino]-BODIPY, and evaluated its photophysical properties and  $\text{Cu}^{2+}$ -sensing ability.

## 2. Materials and Methods

### 2.1. Synthesis of BODIPY 1

Unless otherwise stated, all reagents were purchased from Sigma-Aldrich (St. Louis, MO, USA), Wako Pure Chemical Industries (Osaka, Japan), or Tokyo Chemical Industry (Tokyo, Japan), and used without further purification. Figure 1 shows the synthetic route to BODIPY 1. High-performance thin-layer chromatography (HPTLC; silica gel 60 F<sub>254</sub>, Merck KGaA, Darmstadt, Germany) or thin-layer chromatography (aluminum oxide 60 F<sub>254</sub>, basic, Merck KGaA, Darmstadt, Germany) were used to monitor the reactions. HPTLC plates were visualized under ultraviolet light and/or by staining with anisaldehyde solution (anisaldehyde/ethanol/sulfuric acid/acetic acid = 1.9/68/2.5/1.2, *v/v*), followed by heating for a few minutes. Silica gel 60 (230–400 mesh) or aluminum oxide 90 active basic (Merck KGaA, Darmstadt, Germany) were used for open-column chromatography. <sup>1</sup>H NMR spectra were recorded with a JEOL 400 (400 MHz) spectrometer (JEOL Ltd., Tokyo, Japan) at room temperature. Chemical shifts in the NMR spectra are reported in parts per million, relative to tetramethylsilane as the internal standard (residual  $\text{CHCl}_3$ ; 7.26 ppm). Coupling constants (*J*) are reported in hertz. Splitting patterns are indicated as s, singlet; d, doublet; t, triplet; q, quartet; m, multiplet; brs, broad singlet for <sup>1</sup>H NMR data. High-resolution mass spectroscopy (HRMS) was performed with a Thermo Scientific Exactive (Thermo Fisher Scientific K.K., Tokyo, Japan) or JEOL JMS-T100GCv mass spectrometer (JEOL Ltd., Tokyo, Japan).

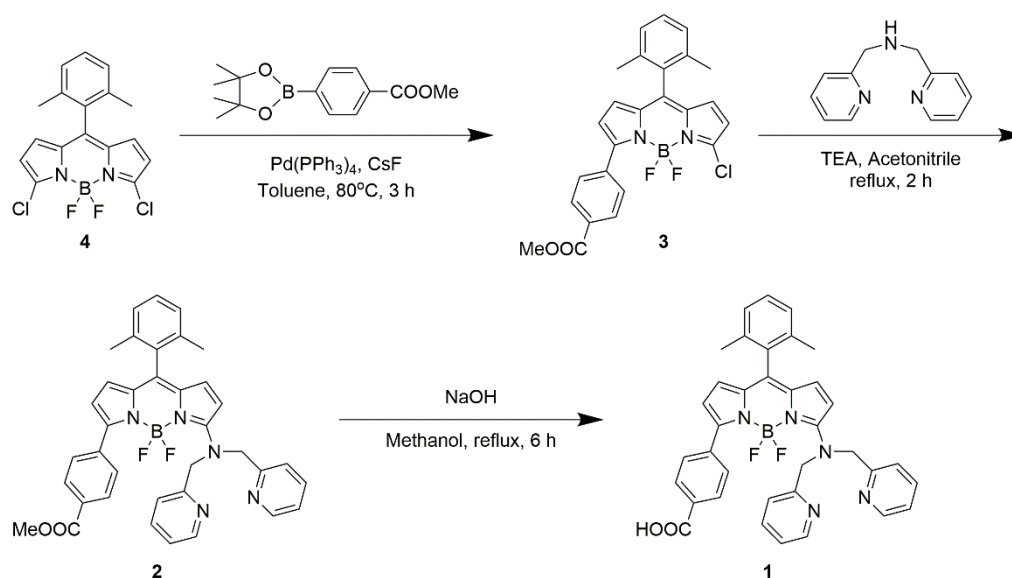


Figure 1. Synthetic route to BODIPY 1.

### 2.1.1. 3-Chloro-4,4-difluoro-5-[4-(methoxycarbonyl)phenyl]-8-(2,6-dimethylphenyl)-4-bora-3a,4a-diaza-s-indacene (3)

Compound 4 was synthesized according to the previously reported method [17]. Compound 4 (120 mg, 0.33 mmol, 1 equiv), 2-(4-methoxycarbonylphenyl)-4,4,5,5-tetramethyl-1,3,2-dioxaborolane (86 mg, 0.33 mmol, 1 equiv), cesium fluoride (150 mg, 0.99 mmol, 3 equiv), and tetrakis (triphenylphosphine)palladium (5 mol %) were dissolved in dry toluene. The reaction mixture was stirred at 80 °C for 3 h under nitrogen. The mixture was cooled to room temperature, water was added, and the organic layer was extracted with dichloromethane. The combined organic layers were washed with brine, and then dried over Na<sub>2</sub>SO<sub>4</sub>. The solvent was evaporated and the crude product was purified by column chromatography on silica gel (hexane/ethyl acetate = 8/1) to yield compound 3 (38%) as a dark-red solid. <sup>1</sup>H NMR (400 MHz, CDCl<sub>3</sub>, Figure S1): δ = 8.15 (d, 2H, J = 8.4 Hz), 8.03 (d, 2H, J = 8.4 Hz), 7.31 (t, 1H, J = 7.6 Hz), 7.16 (d, 2H, J = 7.6 Hz), 6.70 (d, 1H, J = 4.3 Hz), 6.65 (d, 1H, J = 4.2 Hz), 6.59 (d, 1H, J = 4.2 Hz), 6.36 (d, 1H, J = 4.2 Hz), 3.95 (s, 3H), 2.19 (s, 6H). HRMS (ESI, Figure S2) *m/z* calcd for [M + Na]<sup>+</sup> C<sub>25</sub>H<sub>20</sub>BClF<sub>2</sub>N<sub>2</sub>O<sub>2</sub>Na 486.1203; found 486.1207.

### 2.1.2. 3-[Bis(pyridin-2-ylmethyl)amino]-4,4-difluoro-5-[4-(methoxycarbonyl)phenyl]-8-(2,6-dimethylphenyl)-4-bora-3a,4a-diaza-s-indacene (2)

Compound 3 (63 mg, 0.14 mmol, 1 equiv) was dissolved in acetonitrile. Di(2-picolyl)amine (41 mg, 0.20 mmol, 1.5 equiv) and triethylamine (0.57 mL, 4.07 mmol, 30 equiv) were then added to the solution. The reaction mixture was refluxed with stirring for 2 h under nitrogen. The mixture was cooled to room temperature, ethyl acetate was added, and the mixture was washed with water and brine. The organic layer was dried over Na<sub>2</sub>SO<sub>4</sub>, and the solvent was evaporated. The crude product was purified by column chromatography on aluminum oxide basic (hexane/ethyl acetate = 1/1) to yield compound 2 (76%) as a dark-red solid. <sup>1</sup>H NMR (400 MHz, CDCl<sub>3</sub>, Figure S3): δ = 8.53 (d, 2H, J = 4.8 Hz), 8.02 (d, 2H, J = 8.2 Hz), 7.92 (d, 2H, J = 8.3 Hz), 7.64 (td, 2H, J = 7.7, 1.7 Hz), 7.34 (d, 2H, J = 7.8 Hz), 7.23 (t, 1H, J = 7.6 Hz), 7.19–7.16 (m, 2H), 7.10 (d, 2H, J = 7.6 Hz), 6.55 (d, 1H, J = 5.1 Hz), 6.44 (d, 1H, J = 3.8 Hz), 6.24 (d, 1H, J = 5.1 Hz), 6.16 (d, 1H, J = 3.8 Hz), 5.20 (s, 4H), 3.91 (s, 3H), 2.18 (s, 6H). HRMS (ESI, Figure S4) *m/z* calcd for [M + Na]<sup>+</sup> C<sub>37</sub>H<sub>32</sub>BF<sub>2</sub>N<sub>5</sub>O<sub>2</sub>Na 649.2546; found 649.2553.

### 2.1.3. 3-[Bis(pyridin-2-ylmethyl)amino]-4,4-difluoro-5-(4-carboxyphenyl)-8-(2,6-dimethylphenyl)-4-bora-3a,4a-diaza-s-indacene (1)

Compound **2** (37 mg, 0.06 mmol) was dissolved in methanol (15 mL). An aqueous solution of sodium hydroxide (0.2 M, 1.5 mL) was then added to the solution. The reaction mixture was refluxed with stirring for 6 h. The mixture was cooled to room temperature, and then the pH was adjusted to between 4 and 5, by adding an aqueous solution of hydrochloric acid (2 M). Ethyl acetate was added and the mixture was washed with water and brine. The organic layer was dried over Na<sub>2</sub>SO<sub>4</sub> and the solvent was evaporated to yield BODIPY **1** (63%) as a dark-red solid. <sup>1</sup>H NMR (400 MHz, CDCl<sub>3</sub>, Figure S5): δ = 8.54 (d, 2H, J = 4.8 Hz), 8.06 (d, 2H, J = 8.4 Hz), 7.94 (d, 2H, J = 8.4 Hz), 7.64 (td, 2H, J = 7.7, 1.7 Hz), 7.37 (d, 2H, J = 8.0 Hz), 7.23 (t, 1H, J = 7.6 Hz), 7.19–7.16 (m, 2H), 7.10 (d, 2H, J = 7.6 Hz), 6.95 (d, 1H, J = 3.0 Hz), 6.56 (d, 1H, J = 5.1 Hz), 6.45 (d, 1H, J = 3.8 Hz), 6.28 (d, 1H, J = 5.1 Hz), 6.17 (d, 1H, J = 3.8 Hz), 5.23 (s, 4H), 2.18 (s, 6H). HRMS (ESI, Figure S6) *m/z* calcd for [M + H]<sup>+</sup> C<sub>36</sub>H<sub>31</sub>BF<sub>2</sub>N<sub>5</sub>O<sub>2</sub>H 613.2570; found 613.2574.

### 2.2. Fluorescence and UV–Vis Spectroscopic Measurements

Fluorescence spectra were recorded with a Hitachi F-7100 fluorescence spectrophotometer (Hitachi High-Technologies Corporation, Tokyo, Japan) and absorption spectra were recorded with a Shimadzu UV-1800 spectrophotometer (SHIMADZU CORPORATION, Kyoto, Japan). Analytical grade acetonitrile was used for all spectroscopic experiments. Stock solution of BODIPY **1** (40 μM) was prepared by dissolving BODIPY **1** in acetonitrile, and stock solutions of cations (300 μM) were prepared by dissolving metallic perchlorate in acetonitrile. Each test sample was prepared by adding an aliquot of the BODIPY **1** and cation stock solutions to a 10 mL volumetric flask, and then diluting the sample with acetonitrile. For measurements of absorption spectra, an appropriate volume of the cation stock solution was added to a reference cell to ensure absorption spectrum of the test solution. The excitation and emission slit widths were both 5.0 nm. The fluorescence quantum yields of the test solution were calculated by comparing the area under the corrected fluorescence spectrum of the test solution with that of an ethanol solution of rhodamine 6G, which has a fluorescence quantum yield of 0.95 [18]. The fluorescence quantum yield of each sample was obtained as

$$\Phi_S = \Phi_R \times S_S/S_R \times A_R/A_S \times (\eta_S/\eta_R)^2, \quad (1)$$

where  $\Phi$  is the fluorescence quantum yield,  $S$  is the integrated area of the fluorescence spectrum,  $A$  is the absorbance at the excitation wavelength,  $\eta$  is the refractive index of the solvent, and the subscripts,  $S$  and  $R$ , refer to the sample and the reference fluorescent dye (i.e., rhodamine 6G), respectively. All spectroscopic measurements were conducted in at least duplicate.

## 3. Results and Discussion

### 3.1. Photophysical Properties of BODIPY **1**

Table 1 shows the photophysical properties of BODIPY **1**. BODIPY **1** showed a broad absorption band at around 503 nm, with a large molar absorption coefficient ( $\epsilon_{503} = 25,000 \text{ M}^{-1} \text{ cm}^{-1}$ ); it also showed a fluorescence peak at 580 nm. The fluorescence quantum yield and the Stokes shift were 0.34 and  $2600 \text{ cm}^{-1}$ , respectively. The absorption and fluorescence maximum wavelengths, molar absorption coefficient, and Stokes shift of BODIPY **1** were comparable to those of a previously reported sulfonylphenyl-substituted BODIPY cation sensor [17]. However, the fluorescence quantum yield of BODIPY **1** was lower than that of the sulfonylphenyl-substituted BODIPY.

**Table 1.** Photophysical properties of BODIPY 1 in acetonitrile.

$\lambda_{\text{abs}}$ (nm)	$\lambda_{\text{flu}}$ (nm)	$\epsilon_{503}$ ( $\text{M}^{-1} \text{cm}^{-1}$ )	$\Phi$ (-)	Stokes Shift ( $\text{cm}^{-1}$ )
503	580	25,000	0.34	2600

### 3.2. Spectroscopic Response of BODIPY 1 toward Metal Cations

Fluorescence and absorption spectroscopic response of BODIPY 1 was investigated with different metal cations to clarify its cation-sensing ability. Figure 2 shows the absorption and fluorescence spectra of BODIPY 1 with and without the respective metal cations (100 equiv). The absorption spectra of BODIPY 1 showed a broad absorption band at around 503 nm. The addition of metal cations caused the spectra to red-shift. The largest red-shift, to 593 nm, was observed on addition of  $\text{Cu}^{2+}$ . Under excitation at 510 nm,  $\text{Zn}^{2+}$  and  $\text{Ni}^{2+}$  enhanced the fluorescence intensity of BODIPY 1, and the fluorescence peak was slightly blue-shifted from 580 nm to 574 nm and 579 nm for  $\text{Zn}^{2+}$  and  $\text{Ni}^{2+}$ , respectively. In contrast,  $\text{Co}^{2+}$ ,  $\text{Cd}^{2+}$ , and  $\text{Hg}^{2+}$  weakened the fluorescence intensities of BODIPY 1.  $\text{Fe}^{3+}$  and  $\text{Cu}^{2+}$  induced red-shifts of the fluorescence band of BODIPY 1. In particular, the fluorescence peak of BODIPY 1 at 580 nm underwent a large red-shift to 620 nm on addition of  $\text{Cu}^{2+}$ . Figure 3 is the photos of BODIPY 1 solution with and without the respective metal cations (100 equiv). The changes in absorption and fluorescence color caused by  $\text{Cu}^{2+}$  addition were easily distinguishable by the naked eye. Based on these results, we expected the  $\text{Cu}^{2+}$  selectivity of BODIPY 1, because  $\text{Cu}^{2+}$  induced the largest red-shifts of the fluorescence and the absorption spectra of BODIPY 1. Therefore, the  $\text{Cu}^{2+}$ -sensing ability of BODIPY 1 was investigated in the next step. The fluorescence spectral shift enables ratiometric measurement of  $\text{Cu}^{2+}$  concentrations.

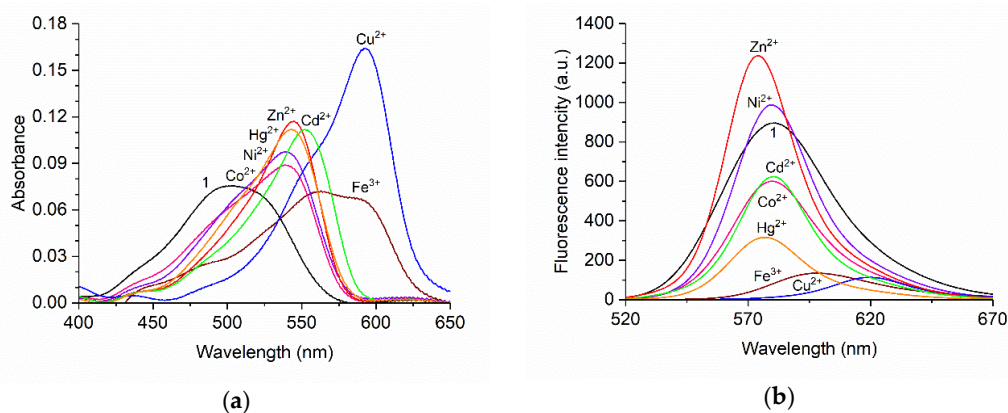


**Figure 2.** (a) Absorption and (b) fluorescence spectra of BODIPY 1 (3  $\mu\text{M}$ ) in the presence of different metal cations (300  $\mu\text{M}$ ) in acetonitrile with excitation at 510 nm.



**Figure 3.** Photos of BODIPY 1 solution (3  $\mu\text{M}$ ) in the presence of different metal cations (300  $\mu\text{M}$ ) in acetonitrile. The fluorescence color was observed under excitation at 365 nm.

### 3.3. Ratiometric Determination of $\text{Cu}^{2+}$ with BODIPY 1

Table 2 shows the photophysical properties of BODIPY 1 in the presence of  $\text{Cu}^{2+}$  (10 equiv). On addition of  $\text{Cu}^{2+}$ , the absorption peak red-shifted from 503 nm to 593 nm and the fluorescence peak red-shifted from 580 nm to 620 nm. Such red-shifted spectra were also observed for previously reported BODIPY sensors with structural similarities to BODIPY 1 [10,12]. The fluorescence quantum yield decreased from 0.34 to 0.07. The absorption and fluorescence spectra of BODIPY 1 with a variety of  $\text{Cu}^{2+}$  concentrations in acetonitrile are shown in Figure 4. In the absorption spectra, the absorption peak was red-shifted by the addition of 1 and 2 equiv of  $\text{Cu}^{2+}$ . On addition of 3 equiv of  $\text{Cu}^{2+}$ , a new absorption peak appeared at 593 nm, and its intensity gradually increased with increasing  $\text{Cu}^{2+}$  concentration. In the fluorescence spectra, the intensity of the fluorescence band at around 580 nm increased on addition of 1 and 2 equiv of  $\text{Cu}^{2+}$ . On addition of 3 equiv of  $\text{Cu}^{2+}$ , a new fluorescence peak appeared at 620 nm, and its intensity gradually increased with increasing concentration of  $\text{Cu}^{2+}$ . Absorption and fluorescence spectral changes almost stopped on addition of 10 equiv of  $\text{Cu}^{2+}$ . These results indicate that the stoichiometry of the BODIPY 1/ $\text{Cu}^{2+}$  complex changes during the addition of 1–3 equiv of  $\text{Cu}^{2+}$  (i.e., 1:1, 1:2, and 1:3 complex of BODIPY 1/ $\text{Cu}^{2+}$ ) because more than two absorption peaks were observed. The absorption peak at 593 nm and the fluorescence peak at 620 nm might originate from 1:3 complex of BODIPY 1 and  $\text{Cu}^{2+}$ , because the distinctive spectral changes were observed upon addition of 3 equiv of  $\text{Cu}^{2+}$ . Therefore, we next investigated the stoichiometry of the system.

**Table 2.** Photophysical properties of BODIPY 1 with  $\text{Cu}^{2+}$  (10 equiv) in acetonitrile.

$\lambda_{\text{abs}}$	$\lambda_{\text{flu}}$	$\epsilon_{593}$	$\Phi$
(nm)	(nm)	( $\text{M}^{-1} \text{cm}^{-1}$ )	(-)
593	620	59,000	0.07

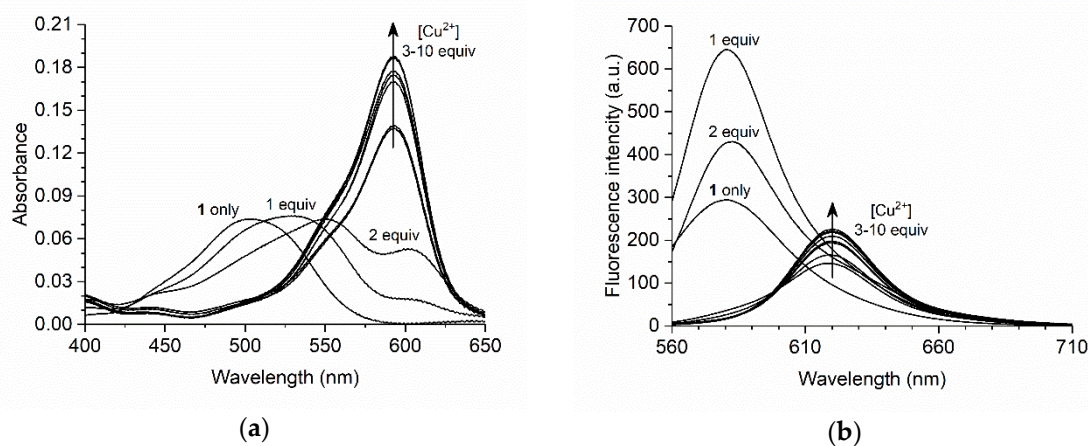


**Figure 4.** Changes in (a) absorption and (b) fluorescence spectra of BODIPY 1 (3  $\mu\text{M}$ ) with increasing  $\text{Cu}^{2+}$  concentration (0–30  $\mu\text{M}$ ) in acetonitrile. The excitation wavelength was 550 nm.

To investigate the binding stoichiometry of BODIPY 1 and  $\text{Cu}^{2+}$ , the Job's method was used [19]. Figure 5a shows the Job's plot of the absorbance at 593 nm ( $A_{593}$ ).  $A_{593}$  was highest when the mole fraction of  $\text{Cu}^{2+}$  was 0.7. The intersection of the fitted lines occurred at approximately 0.75 of the mole fraction of  $\text{Cu}^{2+}$ , suggesting a 1:3 stoichiometry of BODIPY 1 and  $\text{Cu}^{2+}$ . Although we did not introduce the carboxyphenyl group as a cation receptor, the group and acetonitrile might participate in the binding event. The ratio of the fluorescence intensity at 620 nm to that at 580 nm ( $F_{620}/F_{580}$ ) was calculated for ratiometric determination of  $\text{Cu}^{2+}$  (Figure 5b). The  $F_{620}/F_{580}$  value was unchanged in the range 0–6  $\mu\text{M}$   $\text{Cu}^{2+}$  (i.e., 0–2 equiv). In the range 6–15  $\mu\text{M}$   $\text{Cu}^{2+}$ ,  $F_{620}/F_{580}$  increased linearly from 0.4 to

10.8. Further addition of  $\text{Cu}^{2+}$  led to a gradual increase in  $F_{620}/F_{580}$ , and the slope of the plot became low. These results indicate that  $\text{Cu}^{2+}$  concentration can be determined in the range 6–30  $\mu\text{M}$ , and the limit of quantification for  $\text{Cu}^{2+}$  was 6  $\mu\text{M}$ . On the other hand,  $F_{620}$  did not linearly increase depending on the  $\text{Cu}^{2+}$  concentration, which suggests the ratiometric measurement is preferable. To the best of our knowledge, BODIPY 1 is the third example of a ratiometric fluorescent sensor for  $\text{Cu}^{2+}$  based on BODIPY [17,20]. Compared to these sensors, BODIPY 1 shows better quantitative performance for  $\text{Cu}^{2+}$  because the linearity of the calibration curve is well established.

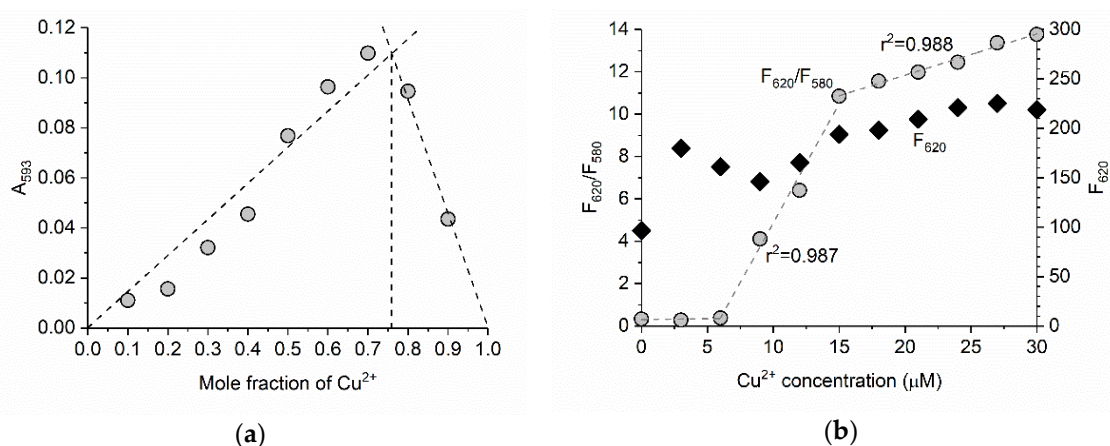


**Figure 5.** (a) Job's plot of BODIPY 1 and  $\text{Cu}^{2+}$  system. The total concentration of BODIPY 1 and  $\text{Cu}^{2+}$  was 9  $\mu\text{M}$  and absorbance at 593 nm ( $A_{580}$ ) was plotted. (b) Plot of fluorescence intensity at 620 nm ( $F_{620}$ ) and ratio of fluorescence intensities ( $F_{620}/F_{580}$ ) of BODIPY 1 (3  $\mu\text{M}$ ) versus increasing  $\text{Cu}^{2+}$  concentration (0–30  $\mu\text{M}$ ) in acetonitrile. The excitation wavelength was 550 nm.

The selectivity of BODIPY 1 for  $\text{Cu}^{2+}$  was investigated (Figure 6a).  $\text{Co}^{2+}$ ,  $\text{Ni}^{2+}$ ,  $\text{Zn}^{2+}$ ,  $\text{Cd}^{2+}$ , and  $\text{Hg}^{2+}$  did not increase the fluorescence intensity at 620 nm, which originated from the complex of BODIPY 1 with  $\text{Cu}^{2+}$ . Addition of the cations, therefore, did not cause  $F_{620}/F_{580}$  to increase. However, when  $\text{Cu}^{2+}$  was added to these solutions,  $F_{620}$  increased and therefore  $F_{620}/F_{580}$  increased. This  $\text{Cu}^{2+}$  selectivity might be a result of the interaction of BODIPY-bis(pyridin-2-ylmethyl)amine conjugate and  $\text{Cu}^{2+}$ , which has a low-lying  $d-d$  state nature [10]. Among these cations,  $\text{Fe}^{3+}$  is the main interfering cation in the use of BODIPY 1 as a  $\text{Cu}^{2+}$  fluorescent sensor, because the fluorescence spectrum of the solution containing 10 equiv of  $\text{Fe}^{3+}$  overlaps with that of the solution containing  $\text{Cu}^{2+}$ . The absorption spectra shown in Figure 2a also suggest the formation of the complex of BODIPY 1 and  $\text{Fe}^{3+}$ . Therefore, some kind of pretreatment for  $\text{Fe}^{3+}$  removal would be necessary for  $\text{Cu}^{2+}$  sensing with BODIPY 1.  $\text{Fe}^{3+}$  also has a paramagnetic nature, and interfering effects for  $\text{Cu}^{2+}$  sensors were often reported [21–23]. To investigate the possibility of practical application for  $\text{Cu}^{2+}$  screening with BODIPY 1, we used tap water (pH = 7.4, electrical conductivity = 19.7 mS/m) as a real sample.  $\text{Cu}^{2+}$  was spiked with tap water, and the concentration of  $\text{Cu}^{2+}$  was adjusted to 30 ppm (470  $\mu\text{M}$ ), which is ten-times higher than the national effluent standards for Cu in Japan. Figure 6b shows the photos of BODIPY 1 solution containing 10% of prepared tap water. The absorption color changed from light pink to light purple by the addition of  $\text{Cu}^{2+}$ . On the other hand, the fluorescence color changed from orange to red purple. Both color changes were easily distinguishable by the naked eye, which is valuable for on-site screening of  $\text{Cu}^{2+}$ .

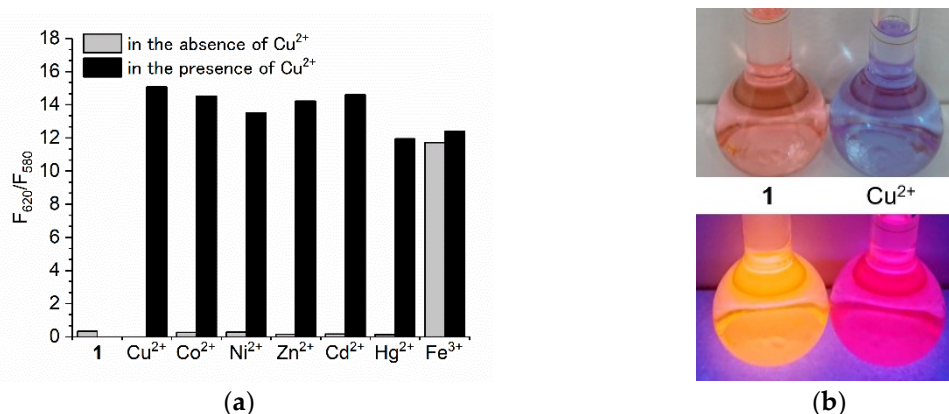


**Figure 6.** (a) Changes in the ratio of fluorescence intensities ( $F_{620}/F_{580}$ ) of BODIPY 1 (3  $\mu\text{M}$ ) on addition of different metal cations. The gray bars represent the addition of each cation (30  $\mu\text{M}$ ). The black bars represent subsequent addition of  $\text{Cu}^{2+}$  (30  $\mu\text{M}$ ). The excitation wavelength was 550 nm. (b) Photos of BODIPY 1 solution (4  $\mu\text{M}$ ) containing tap water (acetonitrile/tap water = 9/1,  $v/v$ ) in the absence (1, left flask) and the presence of  $\text{Cu}^{2+}$  ( $\text{Cu}^{2+}$ , right flask).  $\text{Cu}^{2+}$  was spiked with tap water in advance. The concentration of  $\text{Cu}^{2+}$  in tap water was 30 ppm (470  $\mu\text{M}$ ). The fluorescence color was observed under excitation at 365 nm.

#### 4. Conclusions

In this study, we synthesized BODIPY 1 as a ratiometric fluorescent sensor for  $\text{Cu}^{2+}$ . BODIPY 1 showed large absorption and fluorescence spectral red-shifts on binding to  $\text{Cu}^{2+}$ . The fluorescence quantum yield of the complex was 0.7. The Job's plot revealed 1:3 stoichiometry of BODIPY 1 and  $\text{Cu}^{2+}$ . The ratio of the fluorescence intensity ( $F_{620}/F_{580}$ ) increased with increasing concentration of  $\text{Cu}^{2+}$  (6–30  $\mu\text{M}$ ).  $\text{Fe}^{3+}$  was the main interfering cation for  $\text{Cu}^{2+}$  sensing with BODIPY 1. In addition, BODIPY 1 could be used for  $\text{Cu}^{2+}$  screening in a water-containing sample. The change in fluorescence color by  $\text{Cu}^{2+}$  could be easily recognized by the naked eye.

**Supplementary Materials:** The following are available online at <http://www.mdpi.com/1996-1944/11/5/814/s1>, Figure S1:  $^1\text{H}$  NMR spectrum of compound 3, Figure S2: HRMS spectrum of compound 3, Figure S3:  $^1\text{H}$  NMR spectrum of compound 2, Figure S4: HRMS spectrum of compound 2, Figure S5:  $^1\text{H}$  NMR spectrum of BODIPY 1, Figure S6: HRMS spectrum of BODIPY 1.

**Author Contributions:** A.H., K.Y., and H.S. conceived and designed the experiments. A.H. performed the experiments. A.H., M.T., and S.O. analyzed the data. A.H. and H.S. wrote the paper.

**Funding:** This research was partly supported by a Grant-in-Aid for Scientific Research (KAKENHI Grant Nos. 26289178, 23686074, and 26889054) from the Japan Society for the Promotion of Science.

**Acknowledgments:** We thank Helen McPherson, from Edanz Group ([www.edanzediting.com/ac](http://www.edanzediting.com/ac)) for editing a draft of this manuscript.

**Conflicts of Interest:** The authors declare no conflict of interest.

#### References

1. Gaetke, L.M.; Chow, C.K. Copper toxicity, oxidative stress, and antioxidant nutrients. *Toxicology* **2003**, *189*, 147–163. [[CrossRef](#)]
2. American Public Health Association. *Standard Methods for the Examination of Water and Wastewater*, 22nd ed.; American Public Health Association/American Water Works Association/Water Environment Federation: Washington, DC, USA, 2012; ISBN 9780875530130.
3. Lakowicz, J.R. *Principles of Fluorescence Spectroscopy*, 3rd ed.; Springer: New York, NY, USA, 2006; ISBN 9780387463124.
4. Carter, K.P.; Young, A.M.; Palmer, A.E. Fluorescent sensors for measuring metal ions in living systems. *Chem. Rev.* **2014**, *114*, 4564–4601. [[CrossRef](#)] [[PubMed](#)]

5. Valeur, B.; Berberan-Santos, M.N. *Molecular Fluorescence: Principles and Applications*, 2nd ed.; Wiley-VCH: Weinheim, Germany, 2012; ISBN 9783527328376.
6. Boens, N.; Leen, V.; Dehaen, W. Fluorescent indicators based on BODIPY. *Chem. Soc. Rev.* **2012**, *41*, 1130–1172. [[CrossRef](#)] [[PubMed](#)]
7. Rohand, T.; Qin, W.; Boens, N.; Dehaen, W. Palladium-catalyzed coupling reactions for the functionalization of BODIPY dyes with fluorescence spanning the visible spectrum. *Eur. J. Org. Chem.* **2006**, *2006*, 4658–4663. [[CrossRef](#)]
8. Domaille, D.W.; Zeng, L.; Chang, C.J. Visualizing ascorbate-triggered release of labile copper within living cells using a ratiometric fluorescent sensor. *J. Am. Chem. Soc.* **2010**, *132*, 1194–1195. [[CrossRef](#)] [[PubMed](#)]
9. Hafuka, A.; Taniyama, H.; Son, S.H.; Yamada, K.; Takahashi, M.; Okabe, S.; Satoh, H. BODIPY-based ratiometric fluoroionophores with bidirectional spectral shifts for the selective recognition of heavy metal ions. *Bull. Chem. Soc. Jpn.* **2013**, *86*, 37–44. [[CrossRef](#)]
10. Qin, W.W.; Dou, W.; Leen, V.; Dehaen, W.; Van der Auweraer, M.; Boens, N. A ratiometric, fluorescent BODIPY-based probe for transition and heavy metal ions. *RSC Adv.* **2016**, *6*, 7806–7816. [[CrossRef](#)]
11. Xia, S.; Shen, J.J.; Wang, J.B.; Wang, H.L.; Fang, M.X.; Zhou, H.W.; Tanasova, M. Ratiometric fluorescent and colorimetric BODIPY-based sensor for zinc ions in solution and living cells. *Sens. Actuator B Chem.* **2018**, *258*, 1279–1286. [[CrossRef](#)]
12. Yin, S.; Leen, V.; Van Snick, S.; Boens, N.; Dehaen, W. A highly sensitive, selective, colorimetric and near-infrared fluorescent turn-on chemosensor for Cu<sup>2+</sup> based on BODIPY. *Chem. Commun.* **2010**, *46*, 6329–6331. [[CrossRef](#)] [[PubMed](#)]
13. Zhang, C.L.; Han, Z.; Wang, M.J.; Yang, Z.H.; Ran, X.Q.; He, W.J. A new BODIPY-derived ratiometric sensor with internal charge transfer (ICT) effect: Colorimetric/fluorometric sensing of Ag<sup>+</sup>. *Dalton Trans.* **2018**, *47*, 2285–2291. [[CrossRef](#)] [[PubMed](#)]
14. Chopin, N.; Medebielle, M.; Maury, O.; Novitchi, G.; Pilet, G. Quenching of fluorescence in bodipy-derived trifluoromethyl enamino ligands upon coordination to copper(II). *Eur. J. Inorg. Chem.* **2014**, *2014*, 6185–6195. [[CrossRef](#)]
15. Liu, Z.C.; Yang, Z.Y.; Li, T.R.; Wang, B.D.; Li, Y.; Qin, D.D.; Wang, M.F.; Yan, M.H. An effective Cu(II) quenching fluorescence sensor in aqueous solution and 1D chain coordination polymer framework. *Dalton Trans.* **2011**, *40*, 9370–9373. [[CrossRef](#)] [[PubMed](#)]
16. Razi, S.S.; Srivastava, P.; Ali, R.; Gupta, R.C.; Dwivedi, S.K.; Misra, A. A coumarin-derived useful scaffold exhibiting Cu<sup>2+</sup> induced fluorescence quenching and fluoride sensing (On-Off-On) via copper displacement approach. *Sens. Actuator B Chem.* **2015**, *209*, 162–171. [[CrossRef](#)]
17. Hafuka, A.; Kando, R.; Ohya, K.; Yamada, K.; Okabe, S.; Satoh, H. Substituent effects at the 5-position of 3-bis(pyridine-2-ylmethyl)amino-BODIPY cation sensor used for ratiometric quantification of Cu<sup>2+</sup>. *Bull. Chem. Soc. Jpn.* **2015**, *88*, 447–454. [[CrossRef](#)]
18. Magde, D.; Wong, R.; Seybold, P.G. Fluorescence quantum yields and their relation to lifetimes of rhodamine 6G and fluorescein in nine solvents: Improved absolute standards for quantum yields. *Photochem. Photobiol.* **2002**, *75*, 327–334. [[CrossRef](#)]
19. Connors, K.A. *Binding Constants*, 1st ed.; Wiley-Interscience: New York, NY, USA, 1987; ISBN 9780471830832.
20. Huang, J.L.; Wang, B.; Ye, J.G.; Liu, B.; Qiu, H.Y.; Yin, S.C. A Highly Copper-Selective Ratiometric Fluorescent Sensor Based on BODIPY. *Chin. J. Chem.* **2012**, *30*, 1857–1861. [[CrossRef](#)]
21. Bricks, J.L.; Kovalchuk, A.; Trieflinger, C.; Nofz, M.; Buschel, M.; Tolmachev, A.I.; Daub, J.; Rurack, K. On the development of sensor molecules that display Fe<sup>III</sup>-amplified fluorescence. *J. Am. Chem. Soc.* **2005**, *127*, 13522–13529. [[CrossRef](#)] [[PubMed](#)]
22. He, W.; Liu, Z. A fluorescent sensor for Cu<sup>2+</sup> and Fe<sup>3+</sup> based on multiple mechanisms. *RSC Adv.* **2016**, *6*, 59073–59080. [[CrossRef](#)]
23. Joshi, S.; Kumari, S.; Sarmah, A.; Sakhuja, R.; Pant, D.D. Solvatochromic shift and estimation of dipole moment of synthesized coumarin derivative: Application as sensor for fluorogenic recognition of Fe<sup>3+</sup> and Cu<sup>2+</sup> ions in aqueous solution. *J. Mol. Liq.* **2016**, *222*, 253–262. [[CrossRef](#)]

